

## Raman-scattering study of the high-pressure phase transition in $\text{Cd}_{1-x}\text{Mn}_x\text{Te}$

Akhilesh K. Arora,\* D. U. Bartholomew, D. L. Peterson,<sup>†</sup> and A. K. Ramdas

*Physics Department, Purdue University, West Lafayette, Indiana 47907*

(Received 20 November 1986)

The high-pressure phase transition in  $\text{Cd}_{1-x}\text{Mn}_x\text{Te}$  from the cubic zinc-blende structure to the NaCl structure is investigated by Raman scattering. The measurements are made while increasing as well as decreasing the pressure. The transition pressure depends on composition and shows hysteresis. The behavior of zone-center optical phonons as well as that of zone-boundary acoustic phonons, which appear in the first-order Raman spectra due to the disorder in the mixed crystal, are investigated. The zone-boundary acoustic phonon  $\text{TA}(X)$  shows softening similar to that observed in other compound semiconductors. The longitudinal-optic (LO) phonon frequencies in pure CdTe observed while decreasing pressure match with those observed while increasing pressure whereas in the mixed crystals there is a marked difference. As a result of cycling through the phase transition, the CdTe-like LO-phonon frequencies measured at the ambient pressure are higher compared to those before the cycling; the MnTe-like LO-phonon frequencies show an opposite behavior. This change in the LO-TO splitting of the CdTe-like and MnTe-like modes implies a redistribution of the mode effective charges associated with these modes such that the net charge remains unchanged.

### I. INTRODUCTION

There has been considerable interest in the vibrational spectra of mixed crystals associated with many fundamental aspects of lattice vibrations.<sup>1</sup> Zone-center optical phonons in mixed crystals exhibit one-mode, two-mode, or an intermediate behavior depending on the vibrational characteristics of the end members.<sup>2</sup> In this context, the mixed crystals of the tetrahedrally coordinated II-VI compound semiconductors, where the cation is replaced by a magnetic element like Mn, are of special interest due to their unique combination of semiconducting and magnetic properties.<sup>3</sup> The vibrational spectra of these mixed crystals, known as diluted magnetic semiconductors (DMS's), have been investigated in detail at room pressure.<sup>4,5</sup>

A large number of tetrahedrally coordinated III-V and II-VI compound semiconductors as well as group-IV semiconductors undergo a high-pressure phase transition to the  $\beta$ -Sn metallic phase (body-centered tetragonal) around or above 100 kbar.<sup>6-9</sup> The Cd chalcogenides also undergo the same transition; however, they experience in addition an intermediate transition to an NaCl phase, this transition occurring at a much lower pressure, e.g., in CdTe at 35 kbar.<sup>10</sup> A zone-boundary acoustic phonon has been found to show softening in these compounds<sup>6</sup> and it is speculated that the same phonon is also responsible for driving the phase transition.<sup>8</sup> The optical absorption and luminescence experiments show that the band gap changes from direct to indirect and it has a lower value in the NaCl phase.<sup>11,12</sup> This first-order phase transition is also associated with a large volume change ( $\sim 16\%$ ).<sup>10</sup> Recent optical<sup>13,14</sup> and x-ray<sup>9</sup> measurements show that the DMS  $\text{Cd}_{1-x}\text{Mn}_x\text{Te}$ , a mixed crystal of CdTe and MnTe, also shows similar behavior. A preliminary report of the high-pressure Raman scattering study in this system has been made recently.<sup>15</sup> In the present paper we report a detailed high-pressure Raman scattering investigation of

this phase transition in  $\text{Cd}_{1-x}\text{Mn}_x\text{Te}$  by studying the behavior of the zone-center and zone-boundary phonons as a function of hydrostatic pressure in a diamond anvil cell.

### II. EXPERIMENT

The DMS  $\text{Cd}_{1-x}\text{Mn}_x\text{Te}$  has cubic zinc-blende structure in the composition range  $0 < x < 0.7$ .<sup>4</sup> The samples used in the present investigation were grown by the Bridgman method. Raman scattering measurements at high pressure were carried out in a gasketed diamond anvil cell of National Bureau of Standards design<sup>16</sup> in the backscattering configuration. An Inconel X750 steel gasket with 0.3-mm circular hole was used as the gasket. A 4:1 methanol-ethanol mixture was used as the pressure-transmitting medium. Pressure in the diamond anvil cell was measured by measuring the shifts of ruby  $R$  lines and using the accepted shift<sup>17</sup> of  $-0.753 \text{ cm}^{-1}/\text{kbar}$ . Raman spectra were excited with 100 mW of power from a  $\text{Kr}^+$  laser (7993-, 7525-, 6764-, and 6471-Å lines). A computer-controlled triple monochromator and a standard photon-counting unit was used to analyze the scattered radiation.

### III. RESULTS AND DISCUSSIONS

The mixed crystal  $\text{Cd}_{1-x}\text{Mn}_x\text{Te}$  is known to show a two-mode behavior.<sup>4</sup> A typical Raman spectrum of the mixed crystal for  $x=0.4$  at room pressure in the backscattering configuration is shown in Fig. 1(a). The Raman spectra consist of peaks corresponding to zone-center CdTe-like and MnTe-like transverse-optic (TO) and longitudinal-optic (LO) phonons as well as those associated with the zone-boundary phonons in the low-frequency part of the spectrum. The zone-boundary phonons appear in the first-order Raman spectrum because of the disorder in the mixed crystal.

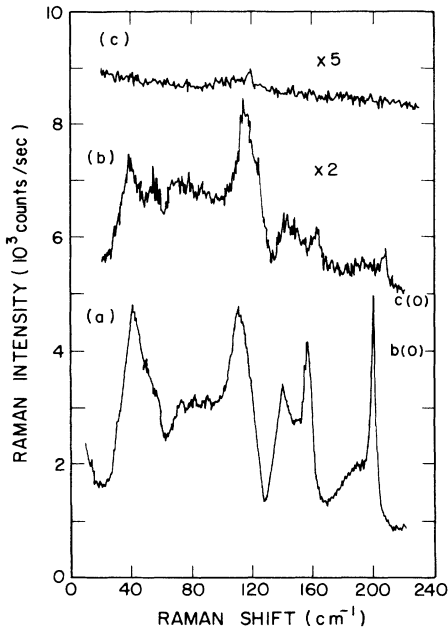


FIG. 1. Raman spectra of  $\text{Cd}_{1-x}\text{Mn}_x\text{Te}$  ( $x=0.4$ ) in back scattering geometry at different hydrostatic pressures: (a) room pressure, (b) 11.1 kbar, and (c) 35.3 kbar. Spectra are vertically displaced for the sake of clarity. The zero intensities for spectra (b) and (c) are marked as  $b(0)$  and  $c(0)$  respectively, on the right-hand vertical scale.

#### A. Zone-center optical phonons

Figures 1(b) and 1(c) show the Raman spectra of  $\text{Cd}_{1-x}\text{Mn}_x\text{Te}$  for  $x=0.4$  at 11.1 and 35.3 kbar, respectively. It can be seen from Fig. 1 that as the hydrostatic pressure is increased, all the zone-center optical phonons shift to higher frequencies and their intensities decrease. All the modes finally disappear as the sample undergoes the phase transition from the cubic zinc-blende to the NaCl phase at 30 kbar. It is well known that the selection rules do not allow any first-order Raman scattering in the NaCl phase. Also, the sample turns opaque to the laser wavelength to which it was transparent in the low-pressure phase. After reaching the NaCl phase if the pressure is now decreased below the forward transition pressure, the Raman intensities do not reappear immediately, but rather at  $19 \pm 3$  kbar suggesting that there is a strong hysteresis associated with the transition. First-order transitions that are associated with large volume changes like the one being investigated here are known to show hysteresis.<sup>10</sup> Mixed crystals with other compositions also show a similar behavior. The pressure dependence of a mode frequency  $\omega_i$  is usually defined in terms of the dimensionless Grüneisen parameter  $\gamma_i$  given by

$$\gamma_i = \frac{1}{\beta \omega_i} \frac{\partial \omega_i}{\partial P}, \quad (1)$$

where  $P$  is the pressure and  $\beta$  the isothermal compressibility. Table I gives the mode Grüneisen parameter of dif-

TABLE I. Mode Grüneisen parameter of zone-center optical phonons in  $\text{Cd}_{1-x}\text{Mn}_x\text{Te}$ . The value of isothermal compressibility is taken from Ref. 9. The numbers in the parentheses give the accuracy of the parameter in the last or the last two significant numbers.

$x$	CdTe-like		MnTe-like	
	TO	LO	TO	LO
0.0		1.01(3)		
0.2	1.61(6)	1.04(5)		1.31(2)
0.4	1.53(12)	1.07(3)	1.29(6)	1.11(2)
0.6	0.93(12)	1.02(7)	1.71(4)	1.15(2)
0.7	-0.14(9)	0.69(5)	1.43(5)	0.94(3)

ferent modes for various compositions of the mixed crystal.

Application of pressure usually changes the band gap and can lead to pressure driven resonance enhancement of the mode intensities.<sup>16</sup> The band gap of  $\text{Cd}_{1-x}\text{Mn}_x\text{Te}$  in the zinc-blende phase is known to increase with pressure.<sup>13</sup> Figure 2 demonstrates the pressure tuning of the resonance enhancement in the case of pure CdTe using the 7993-Å line of the  $\text{Kr}^+$  laser. At room pressure the crystal is opaque to this laser wavelength and the Raman signal due to the LO phonon is weak and rides over a large luminescence background [Fig. 2(a)]. As the pressure is increased the Raman signal increases many fold and the crystal gradually becomes transparent; see Fig. 2(b). At much higher pressures the Raman intensity again drops to very small values [Fig. 2(c) at 26.5 kbar].

Figure 3 compares the Raman spectra of the mixed crystal  $x=0.4$  at room pressure before and after the transition. It can be seen from Fig. 3 that when the pressure is fully released, the Raman spectrum appears quite dif-

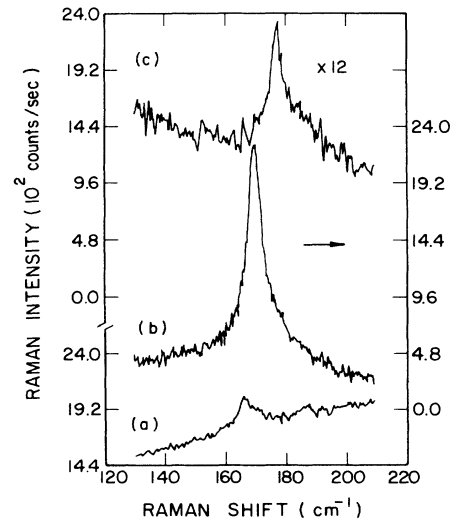


FIG. 2. Resonance enhancement of the LO line in the Raman spectrum of CdTe excited with the 7993-Å line of  $\text{Kr}^+$  laser. The enhancement arises due to the pressure tuning of the band gap. Spectra (a) room pressure, (b) 7.3 kbar, and (c) 26.5 kbar.

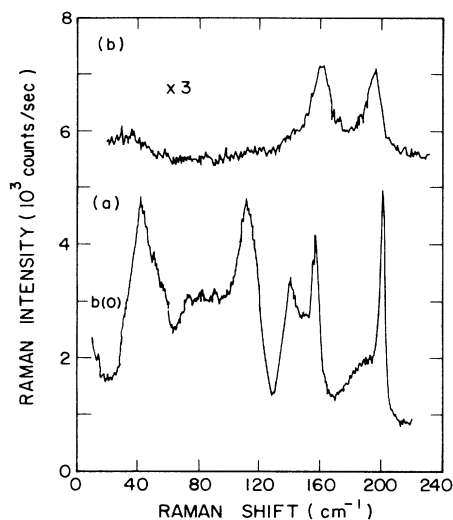


FIG. 3. Raman spectra of  $\text{Cd}_{1-x}\text{Mn}_x\text{Te}$  ( $x=0.4$ ) at room pressure, (a) before and (b) after cycling through the phase transition. The zero intensity for the spectrum (b) is marked as  $b(0)$  on the left-hand vertical axis.

ferent from that at room pressure before the transition. The LO-phonon modes broaden from  $3$  to  $12\text{ cm}^{-1}$  and also shift, whereas TO-phonon and other modes at low frequencies nearly disappear. It is worth pointing out that as the mixed crystal is cycled through the phase transition, it does not remain as a single crystal but shatters and becomes polycrystalline. The presence of defects even in single crystals is known to cause broadening of Raman lines and appearance of a background.<sup>18</sup> Thus the broadening of LO lines and the disappearance of TO and other low-frequency modes into a background could be due to introduction of defects in the process of cycling through the phase transition. Mixed crystals with other compositions also show a similar behavior. Figure 4 shows the behavior of CdTe-like and MnTe-like LO and TO frequencies in the mixed crystals of different compositions while increasing and decreasing the pressure. It can be seen from Fig. 4 that in pure CdTe, LO-phonon frequencies measured with increasing and decreasing pressure match, whereas in the mixed crystals there is a marked difference between them. CdTe-like LO-phonon frequencies, when the crystal is brought back to room pressure after the transition, are higher than those before the transition; MnTe-like LO-phonon frequencies show an opposite trend. Figure 5 shows the composition dependence of the zone-center optical-phonon frequencies at room pressure, before and after the transition. It can be seen from Fig. 5 that the LO-TO splitting of the CdTe-like phonon increases whereas that of the MnTe-like phonon decreases as a result of cycling through the phase transition.

The change in the optical-phonon frequencies as a result of cycling through the phase transition can occur due to one of the following three mechanisms.

(a) The mode frequencies can change if the mixed crystal does not return to the zinc-blende phase after the reverse transition. The zinc-blende phase has only one

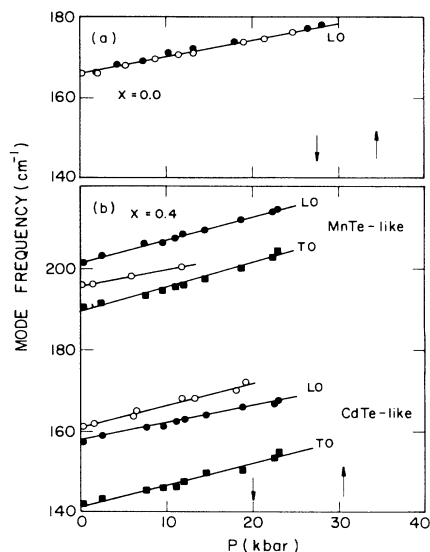


FIG. 4. Zone-center optical phonon frequencies as a function of pressure while increasing as well as decreasing the pressure. (a)  $x=0.0$  and (b)  $x=0.4$ . Circles, LO phonon; squares, TO phonon. Solid symbols, increasing pressure; open symbols, decreasing pressure. Vertical up and down arrows indicate the forward and reverse transitions. Straight lines through the points are the linear least-squares fits to the data.

Raman-active phonon whereas other structures may have a larger number of Raman-active phonons; however, we do not see new lines in the Raman spectra. Also, the most recent x-ray study of this system does not indicate the appearance of a new phase below the reverse transition pressure.<sup>9,19</sup>

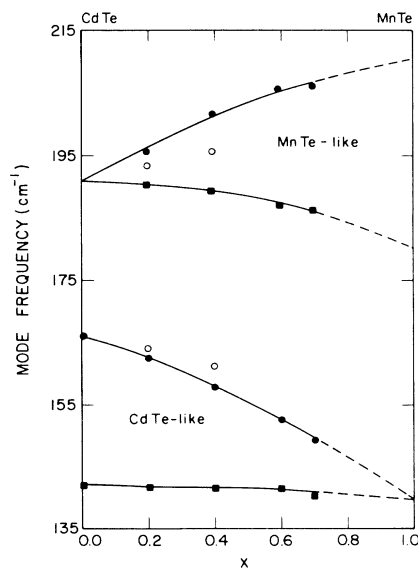


FIG. 5. Composition dependence of CdTe-like and MnTe-like LO (circles) and TO (squares) phonon frequencies at room pressure before (solid symbols) and after (open symbols) cycling through the transition. Solid and dashed lines through the points are only guides to the eye.

(b) A change in the LO-TO splitting can occur if there is a pressure-induced phase separation of the mixed crystal into pure MnTe and  $\text{Cd}_{1-x}\text{Mn}_x\text{Te}$  with a lower  $x$  value. However, if one considers the case of 40%  $\text{Cd}_{1-x}\text{Mn}_x\text{Te}$ , the phonon frequencies after the reverse transition suggest that (see, for example, Fig. 5) the mixed crystal should "phase separate" into 20%  $\text{Cd}_{1-x}\text{Mn}_x\text{Te}$  and the rest of the 20% volume should be pure MnTe having either a hexagonal NiAs structure or a metastable zinc-blende structure. A volume of 20% is too large to remain undetected either in a Raman or a x-ray measurement. The Raman spectra do not show new Raman lines associated with the separated MnTe phase. The recent x-ray measurements have also not indicated any such pressure-induced phase separation.<sup>9,19</sup>

(c) A change in the LO-TO splitting could also mean a redistribution of the mode effective charges because the LO-TO splitting of a mode is determined by the oscillator strength of the mode which in turn depends on the ionicity or the effective charge on the ions in the crystal known as Szigeti effective charge.<sup>2</sup> Another equivalent quantity known as Born's transverse dynamic charge, which is also a measure of ionicity of crystal,<sup>6</sup> is also frequently used in the literature. The present results thus indicate that there could be a redistribution of the effective charge between the CdTe-like and MnTe-like modes when the mixed crystal is cycled through the phase transition. In order to verify this it is of interest to make quantitative estimates of the oscillator strengths and effective charges associated with the CdTe-like and MnTe-like phonons.

In the case of a crystal with two polar modes as in  $\text{Cd}_{1-x}\text{Mn}_x\text{Te}$ , one can write the frequency-dependent dielectric constant as the sum of the individual contributions as

$$\frac{\epsilon(\omega)}{\epsilon_\infty} = 1 + \frac{\omega_{T1}^2 4\pi\rho_1 / \epsilon_\infty}{\omega_{T1}^2 - \omega^2} + \frac{\omega_{T2}^2 4\pi\rho_2 / \epsilon_\infty}{\omega_{T2}^2 - \omega^2}, \quad (2)$$

where subscripts 1 and 2 correspond to CdTe-like and MnTe-like modes and  $4\pi\rho_{1,2}$  are the oscillator strengths. The oscillator strengths of the individual modes can be obtained from Eq. (2) in terms of LO and TO frequencies as<sup>2</sup>

$$\frac{4\pi\rho_1}{\epsilon_\infty} = \frac{(\omega_{L1}^2 - \omega_{T1}^2)(\omega_{L2}^2 - \omega_{T1}^2)}{\omega_{T1}^2(\omega_{T2}^2 - \omega_{T1}^2)} \quad (3a)$$

and

$$\frac{4\pi\rho_2}{\epsilon_\infty} = \frac{(\omega_{L2}^2 - \omega_{T2}^2)(\omega_{L1}^2 - \omega_{T2}^2)}{\omega_{T2}^2(\omega_{T1}^2 - \omega_{T2}^2)}. \quad (3b)$$

We emphasize that in the case of a mixed crystal the oscillator strengths and hence the LO and TO frequencies depend on the composition of the mixed crystal.

When the samples are brought back to room pressure after the transition, the TO phonons are not observed and their values at room pressure after the reverse transition are not known experimentally. However, they can be estimated as follows. In a mixed polar crystal, the splitting of the fundamental vibration frequencies into TO and LO modes is governed by the effective charge<sup>20</sup> which in turn

is reflected in the compositional dependence of the TO and LO frequencies. From Fig. 5 one notices that the TO frequencies show a much weaker composition dependence than do the LO frequencies. As a first step one can estimate the change in TO frequencies due to the changes in the mode effective charges by assuming that the ratio of the change in  $\omega_{TO}$  to that in  $\omega_{LO}$  is governed by ratio of the slopes of the composition dependence of TO and LO frequencies. The composition dependence of the oscillator strengths thus obtained are shown in Fig. 6. For the pure MnTe having a hypothetical zinc-blende structure the LO and TO frequencies were taken from the calculations of the modified random element isodisplacement model.<sup>5</sup> It can be seen from Fig. 6 that the oscillator strengths do change as a result of cycling through the transition. It is interesting to note that the sum of the two oscillator strengths remains unchanged within the experimental error. If the changes in TO frequencies are taken to be more than what has been assumed above, one would conclude that the total oscillator strength has reduced as a result of cycling through the transition, implying a net increase in the covalency.

It is also important to estimate the effective charges associated with the CdTe-like and the MnTe-like modes which directly indicate the ionicity of the mixed crystal. In the formalism discussed by Genzel *et al.*,<sup>2</sup> the effective charge (Szigeti charge,  $q$ ) is related to  $4\pi\rho$  as

$$\left(\frac{q_j(x)}{e}\right)^2 = \left(\frac{3}{\epsilon_\infty + 2}\right)^2 \frac{\epsilon_\infty V(x) f(x)}{4\pi e^2} \frac{4\pi\rho_j}{\epsilon_\infty}, \quad (4)$$

where  $j=1$  (2) implies a CdTe- (MnTe-) like mode, and the volume of the primitive cell ( $V$ ) and the force constant ( $f = \mu\omega_T^2$ ) are composition dependent. The lattice parameter and the force constant are taken to vary linearly with  $x$ . The value of  $\epsilon_\infty$  is taken to be independent of  $x$ . Figure 7 shows the composition dependencies of the estimated effective charges  $q_j/e$  associated with the CdTe-like and MnTe-like modes at room pressure before and after

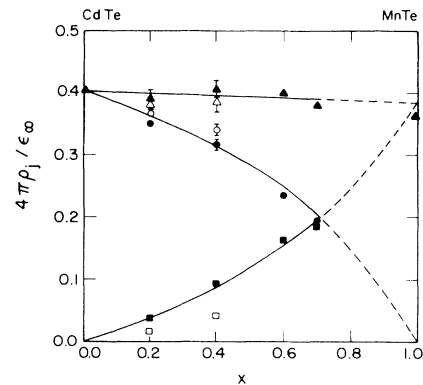


FIG. 6. Composition dependence of the total and the individual oscillator strengths at room pressure before and after cycling through the transition. Triangles, total oscillator strength; circles, CdTe-like mode; squares, MnTe-like mode. Solid symbols, before transition; open symbols, after transition. The solid and dashed lines are only guides to the eye.

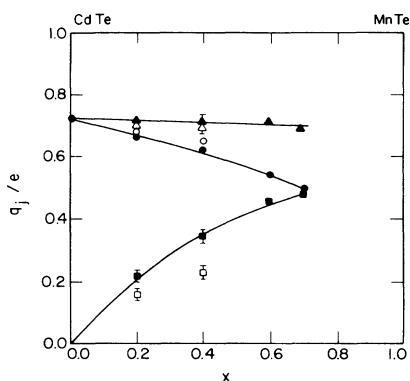


FIG. 7. Composition dependence of the total charge (triangles) and the mode effective charges associated with CdTe-like, circles, and MnTe-like, modes at room pressure before (solid symbols) and after (open symbols) cycling through the transition. Solid lines are only guides to the eye.

cycling through the transition. The total effective charge, which is obtained from the total oscillator strength using Eq. (4), is also shown in the same figure. It is interesting to note that the total charge and hence the ionicity does not vary significantly over the entire composition range of the mixed crystal; however, the mode effective charges vary with the composition as expected. One can see that the mode effective charges are indeed redistributed as a result of cycling the mixed crystal through the phase transition such that the total charge remains unaltered. However, as pointed out earlier, if the changes in the TO frequencies are taken to be more than predicted by their composition dependence, the net ionicity would reduce as a result of cycling through the transition. Although the physical cause of the redistribution of charge is not clear, we speculate that it is due to the evolution of a new local order as a result of rearrangement of atoms occurring during the cycling through the transition.

The effective charge and hence the ionicity is known to decrease as a function of pressure in a number of com-

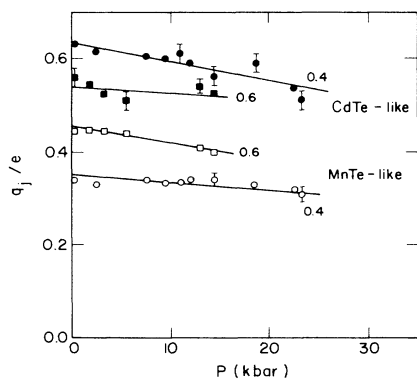


FIG. 8. Pressure dependence of effective charge associated with CdTe-like (solid symbols) and MnTe-like (open symbols) modes for  $x=0.4$ , circles, and  $x=0.6$ , squares. Straight lines through the points are only guides to the eye.

pound semiconductors.<sup>6,21</sup> However, the behavior of mode effective charges in mixed crystals as a function of pressure has not been investigated earlier. It is interesting to note in Fig. 8 that the slope of  $q_j/e$  versus pressure for MnTe-like mode is lower than that for CdTe-like mode for  $x=0.4$ , whereas for  $x=0.6$  the trend is reversed. This reversal of the behavior of CdTe-like and MnTe-like modes is a result of the exchange of the roles of the “host” and the “impurity” in the two cases.

### B. Zone-boundary phonons

As stated earlier, the zone-boundary phonons appear in the first-order Raman spectra due to the disorder in the mixed crystal. From Figs. 1(a) and 1(b), one can see that the low-frequency part of the spectrum consists of three main peaks—at 42, 72, and 112  $\text{cm}^{-1}$ . From the knowledge of the phonon dispersion curves and one-phonon density of states in pure CdTe,<sup>22</sup> the peak at 42  $\text{cm}^{-1}$  has been assigned to  $\text{TA}(X)$ .<sup>5</sup> The temperature dependence of the peak at 72  $\text{cm}^{-1}$  suggested that it is a  $\text{LA}(L)\text{-TA}(L)$ .<sup>23</sup> Though the position of the peak at 112  $\text{cm}^{-1}$  coincides with that  $\text{LA}(L)$ , its shape and polarization has led Venugopalan *et al.*<sup>4</sup> to assign it to a disorder-activated breathing mode of Te around a cation.

The behavior of these three modes as a function of pressure is shown in Fig. 9. It can be seen that the zone-boundary phonon  $\text{TA}(X)$  and the mode at 72  $\text{cm}^{-1}$  show softening whereas the one at 112  $\text{cm}^{-1}$  shows a more complex behavior. Table II gives  $\gamma$  for zone-boundary modes for different compositions.  $\text{TA}(X)$  has been identified as a soft mode<sup>8</sup> for the cubic zinc-blende to  $\beta\text{-Sn}$  transition in a number of II-VI and III-V compound semiconductors. In  $\text{Cd}_{1-x}\text{Mn}_x\text{Te}$ , including pure CdTe, the transition to  $\beta\text{-Sn}$  structure takes place at 110 kbar.<sup>9</sup> It has been suggested that the  $\gamma$  for  $\text{TA}(X)$  varies linearly with the transition pressure in a number of II-VI compound semiconductors as well as in Si and GaP; however, the recent results on GaAs and InP do not seem to follow this trend. The value of  $\gamma$  for  $\text{TA}(X)$  in this system has a

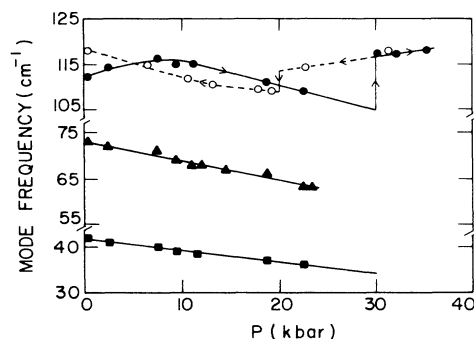


FIG. 9. Pressure dependence of the zone-boundary phonon and the defect-mode frequencies in  $\text{Cd}_{1-x}\text{Mn}_x\text{Te}$  ( $x=0.4$ ). Squares,  $\text{TA}(X)$ ; triangles, 72- $\text{cm}^{-1}$  line; circles, disorder activated breathing mode of Te around a cation. Open symbols correspond to the decreasing pressure. Straight lines through the squares and triangles are linear least-squares fits to the data. The curves through the circles are only guides to the eye.

TABLE II. Mode Grüneisen parameter of zone-boundary phonons and defect mode in  $\text{Cd}_{1-x}\text{Mn}_x\text{Te}$ . The value of the isothermal compressibility is taken from Ref. 9. The numbers in the parentheses give the accuracy of the parameter in the last significant number.

$x$	TA( $X$ )	72-cm <sup>-1</sup> mode	Breathing mode
0.2	-1.8(1)	-2.6(1)	2.9(3)
0.4	-2.4(1)	-2.3(1)	2.5(3)
0.6			2.1(3)
0.7	-2.6(1)		0.4(3)

value  $-2.4$ , while the expected value from the linear relation<sup>8</sup> at 110 kbar, the transition pressure from NaCl phase to  $\beta$ -Sn phase, turns out to be  $-1.5$ . Hence as in the case of InP and GaAs, this system also does not obey the rule proposed by Weinstein<sup>8</sup> for the phase transition in zincblende semiconductors; however, it is interesting to note that if the pressure dependence of TA( $X$ ) mode in  $\text{Cd}_{1-x}\text{Mn}_x\text{Te}$  is extrapolated linearly beyond the zincblende to NaCl transition pressure, the mode frequency goes to zero at a pressure close to that of the transition from the NaCl phase to the  $\beta$ -Sn phase. The significance of this observation in the context of the TA( $X$ ) being the soft mode for the transition to  $\beta$ -Sn phase needs further examination.

If the peak at 72 cm<sup>-1</sup>, which shows softening, is assigned to the LA( $L$ )-TA( $L$ ) difference mode, this would imply that LA( $L$ ) also shows softening because TA( $L$ ) phonon is expected to show softening similar to that of TA( $X$ ) phonon.<sup>6</sup> However, LA( $L$ ) phonon in a number of other tetrahedrally coordinated compound semiconductors is known to have a positive  $\gamma$  with a value close to unity<sup>21</sup> thus making controversial the previous assignment of the 72-cm<sup>-1</sup> mode to the LA( $L$ )-TA( $L$ ) mode.

We draw attention to the mode at 112 cm<sup>-1</sup> which shows a more complex behavior than those of the zone-center optical phonons or the zone-boundary acoustic phonon (Fig. 9). The previous assignment of this mode to the disorder-activated breathing mode of Te around a cation<sup>4</sup> is in agreement with the present observation. The mode frequency for  $x=0.4$  increases with pressure ini-

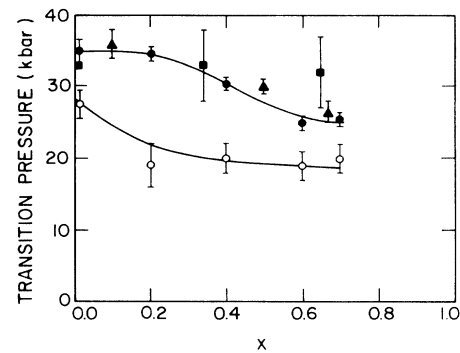


FIG. 10. Composition dependence of the forward, solid symbols, and reverse, open symbols, transition pressures. Circles, present work; squares, x-ray measurements (Ref. 9); triangles, optical-absorption measurements (Ref. 13).

tially and then shows softening. It could be followed beyond the transition pressure in the NaCl phase, and shows discontinuous changes across the forward and reverse transitions. The hysteresis associated with the transition is clearly seen. The mode frequency in the zincblende phase after the reverse transition shows a pressure dependence different from that before the transition. The origin of this behavior is not clear.

Finally, Fig. 10 shows the composition dependence of the forward and the reverse transition pressures. The values reported from the x-ray<sup>9</sup> and the optical-absorption<sup>13</sup> measurements are also shown for comparison. There is a good agreement between the values obtained from different techniques. Both the forward and the reverse transition pressures do show a significant composition dependence as predicted.<sup>24</sup>

#### ACKNOWLEDGMENTS

Authors are indebted to A. Jayaraman for initiating them into the art and science of the diamond anvil cell. They acknowledge valuable discussions with him, Manuel Cardona, and Sergio Rodriguez. The work reported in this paper has been supported by the National Science Foundation under Grant No. DMR 8520866.

\*On leave from Materials Science Laboratory, Reactor Research Centre, Kalpakkam 603102, India.

†Present address: Kodak Research Laboratory, Eastman Kodak Company, Rochester, NY 14650.

<sup>1</sup>A. S. Barker, Jr. and A. J. Sievers, *Rev. Mod. Phys.* **47**, Suppl. No. 2(1975).

<sup>2</sup>L. Genzel, T. P. Martin, and C. H. Perry, *Phys. Status Solidi B* **62**, 83 (1974).

<sup>3</sup>J. K. Furdyna, *J. Appl. Phys.* **53**, 7637 (1982).

<sup>4</sup>S. Venugopalan, A. Petrou, R. R. Galazka, A. K. Ramdas, and S. Rodriguez, *Phys. Rev. B* **25**, 2681 (1982).

<sup>5</sup>D. L. Peterson, A. Petrou, W. Giriat, A. K. Ramdas, and S. Rodriguez, *Phys. Rev. B* **33**, 1160 (1986).

<sup>6</sup>R. Trommer, H. Muller, M. Cardona, and P. Vogl, *Phys. Rev.*

*B* **21**, 4869 (1980).

<sup>7</sup>B. A. Weinstein, in *Proceedings of the 13th International Conference on Physics of Semiconductors, Rome, 1976*, edited by F. G. Fumi (Tipografia Marves, Rome, 1976), p. 326.

<sup>8</sup>B. A. Weinstein, *Solid State Commun.* **24**, 595 (1977).

<sup>9</sup>K. Strossner, S. Ves, W. Dieterich, W. Gebhardt, and M. Cardona, *Solid State Commun.* **56**, 563 (1985).

<sup>10</sup>C. F. Cline and D. R. Stephens, *J. Appl. Phys.* **36**, 2869 (1965).

<sup>11</sup>J. R. Mei and V. Lemos, *Solid State Commun.* **52**, 785 (1984).

<sup>12</sup>B. Batlogg, A. Jayaraman, J. E. Van Cleve, and R. G. Maines, *Phys. Rev. B* **27**, 3920 (1983).

<sup>13</sup>W. Shan, S. C. Shen, and H. R. Zhu, *Solid State Commun.* **55**, 475 (1985).

- <sup>14</sup>E. Muller, W. Gebhardt, and W. Rehwald, *J. Phys. C* **16**, L1114 (1983).
- <sup>15</sup>A. K. Arora, D. U. Bartholomew, D. L. Peterson, and A. K. Ramdas, in *Proceedings of the Tenth International Conference on Raman Spectroscopy, Eugene Oregon, 1986*, edited by W. L. Peticolas and B. Hudson (Oregon University Press, Eugene, Oregon, 1986), p. 7–15.
- <sup>16</sup>A. Jayaraman, *Rev. Sci. Instrum.* **57**, 1013 (1986).
- <sup>17</sup>G. J. Piermarini and S. Block, *Rev. Sci. Instrum.* **46**, 973 (1975).
- <sup>18</sup>C. Hermann and P. Y. Yu, *Phys. Rev. B* **21**, 3675 (1980).
- <sup>19</sup>M. Cardona (private communication).
- <sup>20</sup>H. Fröhlich, *Theory of Dielectrics* (Oxford University Press, Oxford, 1958), p. 149.
- <sup>21</sup>B. A. Weinstein and R. Zallen, in *Light Scattering in Solids IV*, edited by M. Cardona and G. Güntherodt (Springer-Verlag, Berlin, 1984), p. 463.
- <sup>22</sup>J. M. Rowe, R. M. Nicklow, D. L. Price, and K. Zanio, *Phys. Rev. B* **10**, 671 (1974).
- <sup>23</sup>M. Picquart, E. Amzallag, M. Balkanski, Ch. Julien, W. Gebicki, and W. Nazarewicz, *Phys. Status Solidi B* **99**, 683 (1980).
- <sup>24</sup>P. Maheswaranathan, R. J. Sladek, and U. Debska, *Phys. Rev. B* **31**, 5212 (1985).